

Biophysical Journal, Volume 110

Supplemental Information

The Slow Mobility of the ParA Partitioning Protein Underlies Its Steady-State Patterning in *Caulobacter*

Ivan V. Surovtsev, Hoong Chuin Lim, and Christine Jacobs-Wagner

Supplementary Information

Slow mobility of the ParA partitioning protein underlies its steady-state patterning in *Caulobacter*

Ivan Surovtsev^{1,2,3,†}, Hoong Chuin Lim^{1,4,†,#}, Christine Jacobs-Wagner^{1,2,3,5*}

¹ Microbial Sciences Institute, Yale West Campus, West Haven, CT 06516, USA

² Department of Molecular, Cellular and Developmental Biology, Yale University, New Haven, CT 06520, USA

³ Howard Hughes Medical Institute, Yale University, New Haven, CT 06520, USA

⁴ Department of Molecular Biophysics and Biochemistry, Yale University, New Haven, CT 06520, USA

⁵ Department of Microbial Pathogenesis, Yale School of Medicine, New Haven, CT 06510, USA

† Contributed equally.

Current address: Department of Microbiology and Immunobiology, Harvard Medical School, Boston, USA.

*Corresponding author.

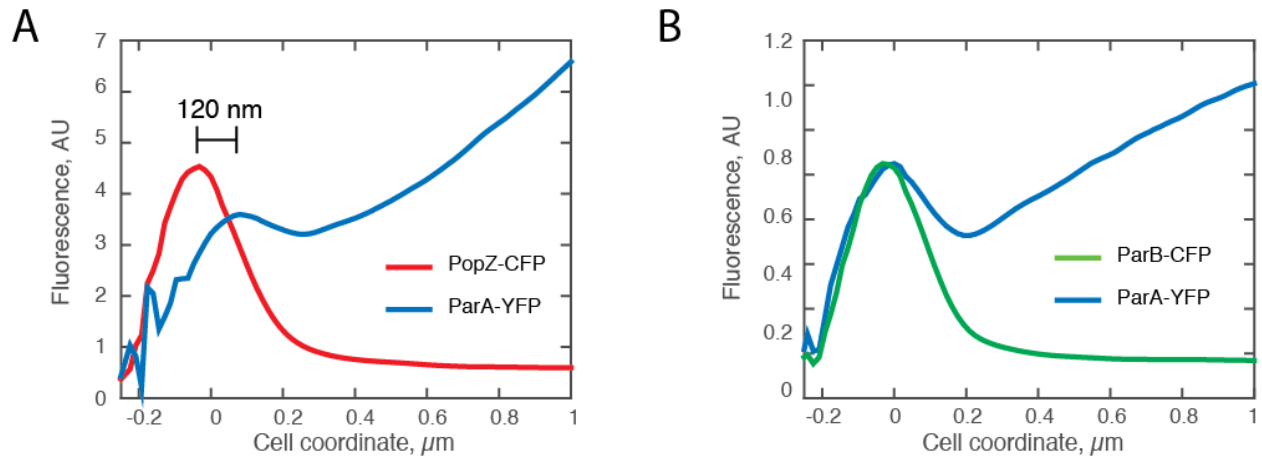


Figure S1. Co-localization of ParA with the PC at the old cell pole of *C. crescentus* swarmer cells. (A) CJW4626 swarmer cells ($n = 230$) expressing PopZ-CFP and ParA-YFP or (B) CJW3367 swarmer cells ($n = 200$) expressing ParB-CFP and ParA-YFP were imaged and the corresponding fluorescence signals were analyzed using Oufiti (17). The pole assignment was based on the asymmetric ParA gradient. To generate the average fluorescence profile, fluorescence profiles of PopZ-CFP and ParA-YFP in CJW4626 swarmer cells and those of ParB-CFP and ParA-YFP in CJW3367 swarmer cells were aligned such that the peak of polar PopZ-CFP or ParB-CFP of each cell was centered at zero on the cell coordinate.

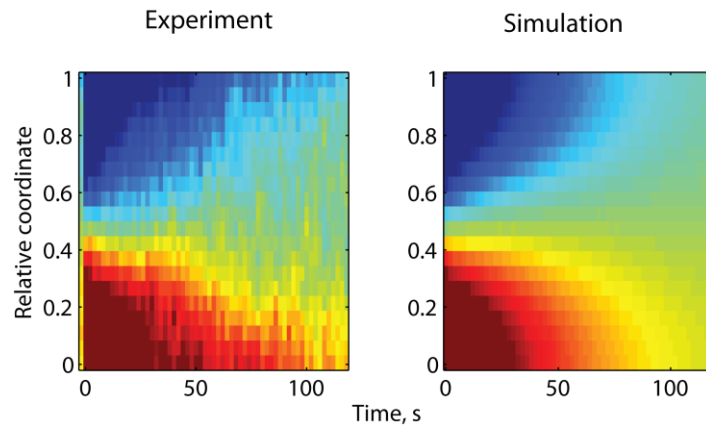


Figure S2. An example of experimental (left) and theoretical (right) kymographs for ParA-CFP recovery after photobleaching in an *E. coli* cell. FRAP experiment was performed on *E. coli* cells expressing *parA-cfp* (CJW3354). The theoretical kymograph was simulated with the best-fit value ($D = 0.005 \mu\text{m}^2/\text{s}$).

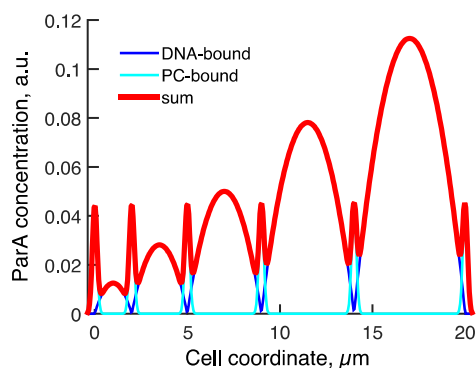


Figure S3. An example of the theoretical distribution of ParA in a filamentous cell with 6 PCs. The theoretical ParA profile for a 20- μm virtual cell containing 6 PCs at $x = 0, 2, 5, 9, 14, 20 \mu\text{m}$ was calculated using Eq. 5c, with $D = 5 \cdot 10^{-3} \mu\text{m}^2 \text{s}^{-1}$ and $k_h = 0.03 \text{s}^{-1}$.

Movie S1. Stochastic 1D simulation showing the evolution of ParA distribution over time. Shown is the average ParA profile (red shade) at selected time points ($n = 500$ simulations). In each simulation, 100 ParA dimers were distributed with uniform probability along the cell coordinate (red dash line). Each ParA dimer was then allowed to diffuse ($D = 5 \cdot 10^{-3} \mu\text{m}^2/\text{s}$), to interact with ParB (green shade) for a period of time governed by $\tau = 1/k_h = 20 \text{s}$ and to redistribute uniformly within the cell following interaction with ParB.

Table S1. Strains used in this study

Name	Relevant genotype or features	Reference
<i>C. crescentus</i> strains		
CB15N	Synchronizable variant of wild-type CB15, also named NA1000	(16)
CJW763	CB15N <i>creS</i> ::Tn5	(39)
CJW2642	CB15N <i>ftsZ</i> ::pBGENTP _{xylftsZ}	Dr. Matthew Cabeen
CJW3040	CB15N <i>parA</i> :: <i>parA-yfp mipZ</i> :: <i>mipZ-cfp</i>	(4)
CJW3367	CB15N <i>parA</i> :: <i>parA-yfp xylX</i> ::pXCFPN-5parB	(4)
CJW4487	CB15N <i>parA</i> :: <i>parA-yfp mipZ</i> :: <i>mipZ-cfp ftsZ</i> ::pBGENTP _{xylftsZ} <i>creS</i> ::Tn5	This study
CJW4626	CB15N <i>parA</i> :: <i>parA-yfp popZ</i> :: <i>popZ-cfp</i>	(20)
<i>E. coli</i> strains		
CJW3354	BL21(λ DE3)/pACYC-ParAeCFP	(4)
CJW3355	BL21(λ DE3)/pACYC-ParAR195EeCFP	(4)
CJW3604	BL21(λ DE3)/pACYC-ParAD44AeCFP	(4)